Journal of Sound and Vibration (1998) **216**(4), 571–583
Article No. sv951714

VIBRO–ACOUSTIC ANALYSIS AND IDENTIFICATION OF DEFECTS IN ROTATING MACHINERY, PART II: EXPERIMENTAL STUDY

N. Hamzaoui, C. Boisson and C. Lesueur

Laboratoire Vibrations Acoustique Bt 303 *INSA*, *Avenue Albert Einstein*, 69621 *Villeurbanne Cedex*, *France*

(*Received* 26 *July* 1995)

The companion paper, Part I, is a theoretical modelling which consists in developing a vibro–acoustic calculation of a rotating rotor on bearings with a numerical simulation of mechanical defects. Controlled error and small computation time distinguish the method. This paper presents the experimental study which was obtained for a test bench composed of three supports (motor, rotor on bearings and speed reducer), in order to simulate such mechanical defects. Comparisons between theoretical and experimental results are presented.

1. INTRODUCTION

In Part I [1], a vibro–acoustic model for a rotor-journal bearings system was presented, the journals being simulated by translational and rotational stiffnesses. Excitation forces applied to this model are those of the main defects encountered in rotating machinery: imbalance and misalignment. The calculation programs developed enables one to determine vibration responses at any point of the vibrating surface and radiated noise levels. Validation tests as well as sensitivity tests were performed on several parameters in order to confirm the hypotheses and simplifications made during the present procedure. Mechanical characteristics of the journals (stiffness, clearance . . .), vibration, measurement consistency (magnitudes and phases . . .), the type of acoustic field and the frequency band analyzed are the most sensitive parameters in this type of calculation. This theoretical approach enables defect configuration simulations by characterizing their vibro–acoustic behaviour and a study of their coupling to be made. This is a helpful step toward defect identification through acoustic analyses, together with vibration analyses, which will aid the development of quieter machines.

The aim of this particular study was to test the validity of the present vibro–acoustic approach by comparing the results with experimental measurements. The authors' experimental installation enables one to simulate different defect configurations in rotating machinery. In this paper, the experimental apparatus is first presented, then the different configurations used during the

0022–460X/98/390571 + 13 $30.00/0

experiment are examined. Finally a comparison is made between theoretical and experimental results.

2. EXPERIMENTAL APPARATUS

A prototype was made based on industrial criteria. This prototype enables both decomposition and a classification of different noise sources to be carried out. This experimental prototype (see Figure 1) consists of three distinct parts: part I, motor; part II, journal; part III, receptor.

Part I is made of a three-phase asynchronous motor (220–380 V, power 4 kW). The rotating speed can vary from 0–6000 r.p.m. It is possible to create both angular and parallel misalignment by a moving set of plates.

Part II consists of two plates which support the journals, one able to rotate only longitudinally and the other translationally. Different journals are available, in order to set up all the bearings associated to the dimension series 206. Different interchangeable elastic settings are also available for linking part I (motor) to part II. This will thus enable the accurate simulation of the vibro–acoustic behaviour of these links. For part I, two balancing discs are mounted on the rotating shaft between the two journals.

Part III consists of a reducing gearbox with a ratio of 1·33 and a direct current generator that can produce a variable resistance torque. Many interchangeable settings are also available for the coupling of part II to part III.

Several gauges (displacement, angular misalignment, and force) are also mounted on the experimental installation and are connected to a monitoring unit. The acoustic isolation of the different noise sources is achieved by overturning the plates. It is therefore possible to simulate different configurations for unbalance, misalignment and defects in gears or bearings.

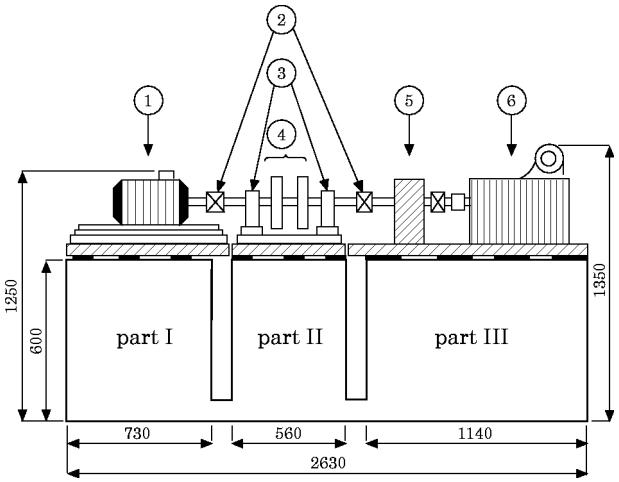

Figure 1. Experimental apparatus: 1, motor; 2, couplings; 3, journals; 4, rotor (shaft + discs); 5, gears; 6, load generator.

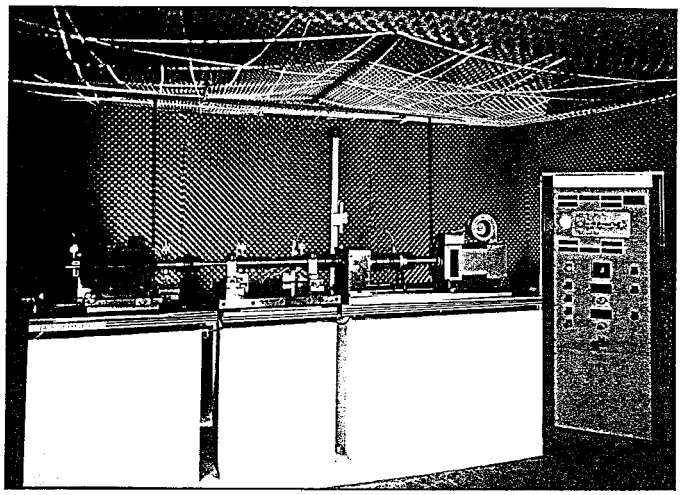

Figure 2. The experimental set-up.

3. TESTS AND RESULTS

One focuses attention on part II by acoustically isolating parts I and III (part III is completely disconnected from part II).

Vibration measurements represented by spectra appearing on the journal bearings are analyzed in the three directions (vertical, horizontal, axial) by using different ranges of frequency analysis.

Honeycombed foam plates are used to create a quiet acoustic background (see Figure 2) in order to acoustically isolate part II. Pressure and acoustic intensity measurements were performed at distinct points located on the horizontal plane and on the two vertical planes surrounding part II. The three surfaces on which the measurements were made coincide with the base of the support of the machine in order to avoid acoustic leaks. It will therefore be possible to assess partial acoustic powers, those relative to each measurement surface, as well as the total acoustic power. An automatic acoustic mesh generator was constructed as the number of measurement points is significant. This mesh generator is a mobile arm holding an intensity sounding line. Two stepper motors, controlled by a computer, move the sounding line in the horizontal or vertical plane.

The system in Figure 3 is composed of a rotor, two discs and ball bearings. It enables one to simulate different types of imbalance (static, dynamic and pure torque) by adding specified masses on to the discs called "imbalance discs". Many combinations involving varying the distance between the two discs, their positions and the number of additional masses, were studied (see Figure 4). The vibration and acoustic variations due to imbalance, angular and parallel misalignment at the journals were studied [2]. Some measurements were taken at different time intervals, as a consequence reference states are relative, and come before the states of simulation.

Misalignment at the journals is generated as follows: on the motor side it is an angular misalignment; on the receptor side, it is a parallel misalignment (see Figure 5).

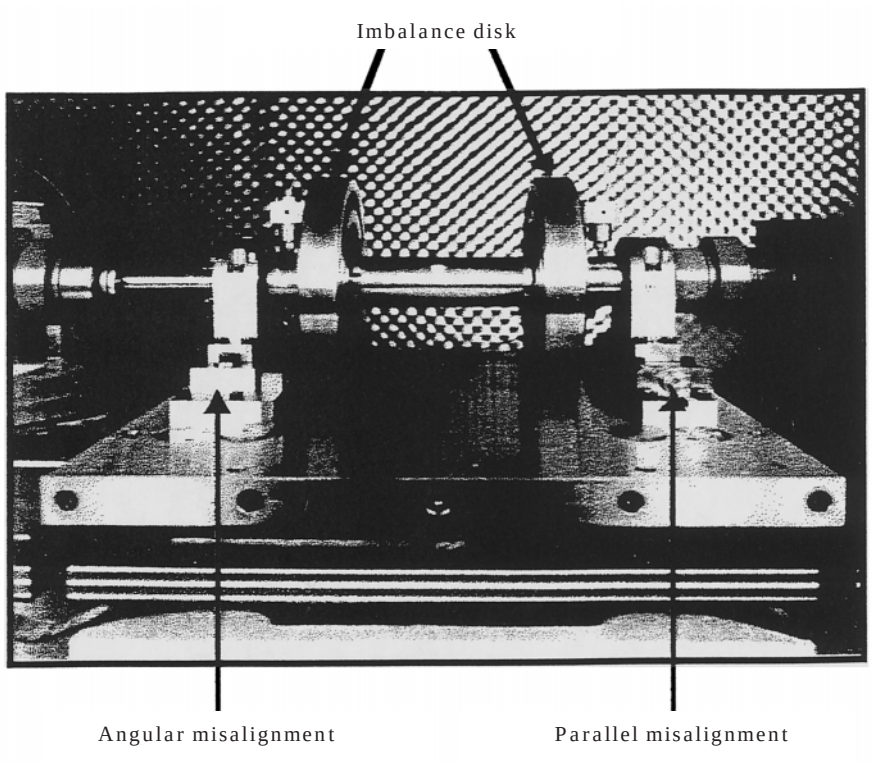

Figure 3. The imbalance disks and angular and parallel misalignment controls.

3.1. DEFECT FREE CONFIGURATION

This step enables the establishment of reference states and validates the experimental apparatus.

At rest, the structure is subjected to individual impacts in order to assess the natural frequencies of its different elements. In the range 0–1000 Hz the two journals have very close natural frequencies in the horizontal direction, the first two, 40 and 62·5 Hz, are due to the variation of the running speed; they may

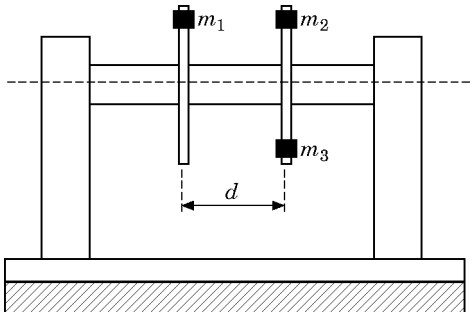

Figure 4. Imbalance simulation: m_1 and m_2, in-phase masses; m_1 and m_3, out-of-phase masses.

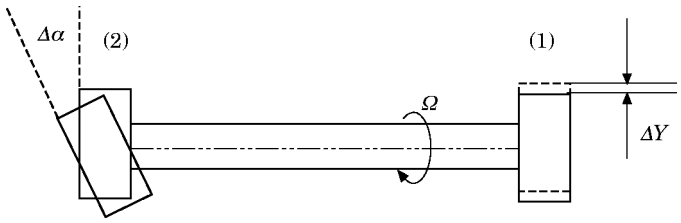

Figure 5. Misalignment between two journal-bearings: (1) parallel; (2) angular.

therefore be amplified. Along the vertical axis, the first natural frequency is greater than 400 Hz; the journals are very stiff in this direction.

At running speed, a spectrum analysis is carried out at the journals. The spectrum obtained is very dense. One can conclude that there is a transmission of vibration energies between the "motor" and "journal" parts at low frequencies through the elastic couplings by demonstrating that there is no transmission through the support. Vibration levels are higher in the horizontal direction than in the others; they also increase with the running speed. The support is the structural element whose vibration energy is the greatest, but on the other hand, if one considers individual measurements, the two journals are predominant.

Acoustic and vibration spectra have the same shape and acoustic pressure levels which significantly increase with the running speed. The ball bearings create a spectrum whose acoustic back spectrum increases when the two "imbalance discs" are present (see Figure 6). By the means of the computer controlled arm which is free to move in the XY plane, from which one obtains an optimal mesh of intensities, the authors were able to calculate the acoustic power. Three sounding lines were used in the frequency range 0–1600 Hz; acoustic power measurements are not reliable below 200 Hz but acoustic pressure spectra are still worth analyzing thoroughly.

Finally when no defect vibrations are present and acoustic levels are low, parasitic noise from the measurement devices becomes very important. The relation between the defects and noise generation is well put forward and should lead to the establishment of criteria of the acoustic quality of a machine.

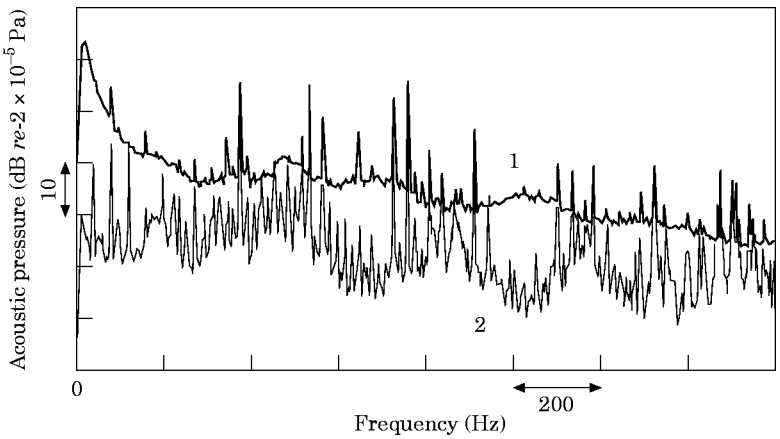

Figure 6. Acoustic pressure level at the same point of 1, the rotor with discs and 2, the rotor without discs.

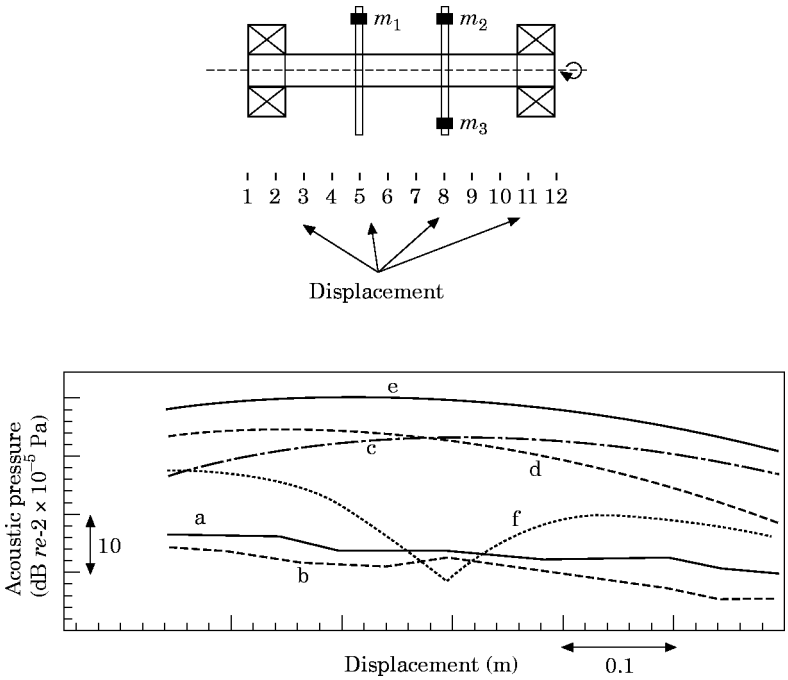

Figure 7. Acoustic pressure level spacial variations measured for different imbalance cases at rotation frequency f_r. (a) Without defects; (b) without defects; (c) imbalance (m_2); (d) imbalance (m_1); (e) imbalance ($m_1 + m_2$); (f) imbalance ($m_1 + m_3$).

3.2. IMBALANCE

Imbalance is generated by adding masses to the disc of the rotor (see Figure 4). One should make distinctions between static imbalance, pure torque, and dynamic imbalance.

The main results are the following: vibration and acoustic levels are strongly amplified at the running frequency whatever the type of imbalance; as far as acoustic pressure is concerned, its level varies in space at running frequency, f_r. Its variations are significant nearer to the added mass (see Figure 7); at frequencies higher than 200 Hz, the spectral variation caused by this defect no longer has a significant influence on the acoustic power (see Figure 8).

3.3. MISALIGNMENT

Misalignment generated at the journals (see Figure 5) is very complex, it is a combination of both angular and parallel misalignment.

The main observations are the following. This defect has no effect on vibration and acoustic levels at the running frequency.

Angular misalignment is characterized by the appearance of components in the spectrum at the kinematical frequencies of the bearings (bearing defect). Pressure levels at such frequencies are high with respect to the reference state near the misaligned bearing. The overall level of acoustic power increases with $\Delta\alpha$ (see Figure 9).

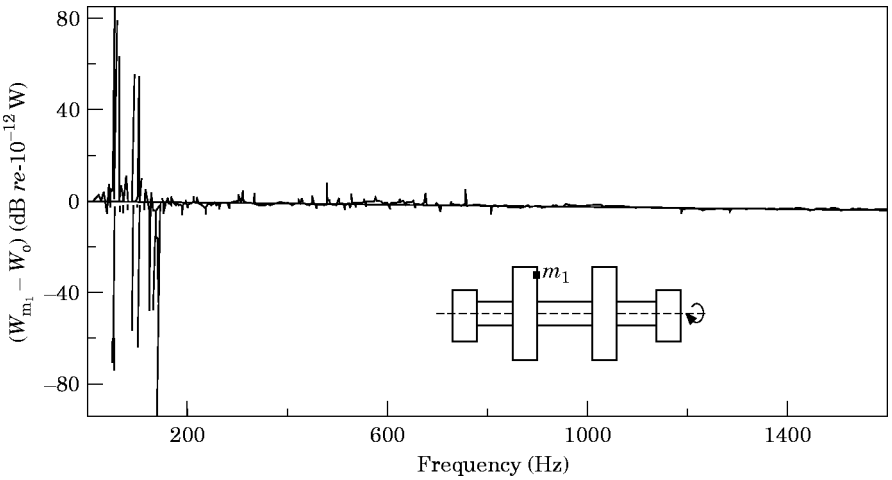

Figure 8. Acoustic power difference between the case with imbalance (m_1) and the case without defect.

It is possible to completely identify vibrations at the journals by considering the transfer function characterized by inertia measurements (acceleration/force). One thus managed to define the force spectrum that represents misalignment at a point of the journal on the "motor" side (see Figure 10). This spectrum also confirms the predominance of the second and fourth harmonics.

4. COMPARISON BETWEEN THEORETICAL AND EXPERIMENTAL RESULTS

In this section, we examine the validity of the theoretical approaches of reference [1] in order to analyze different phenomena and propose criteria for diagnosing defects in rotating machinery.

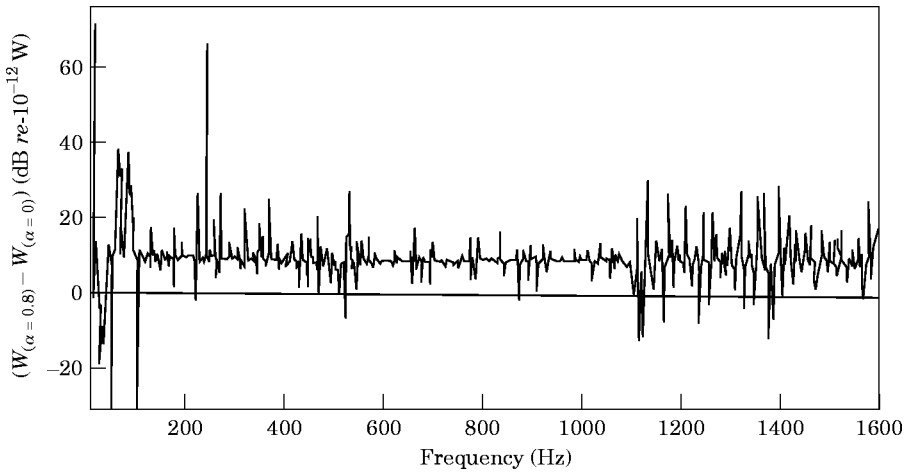

Figure 9. Acoustic power difference between the case with angular misalignment and the case without defect.

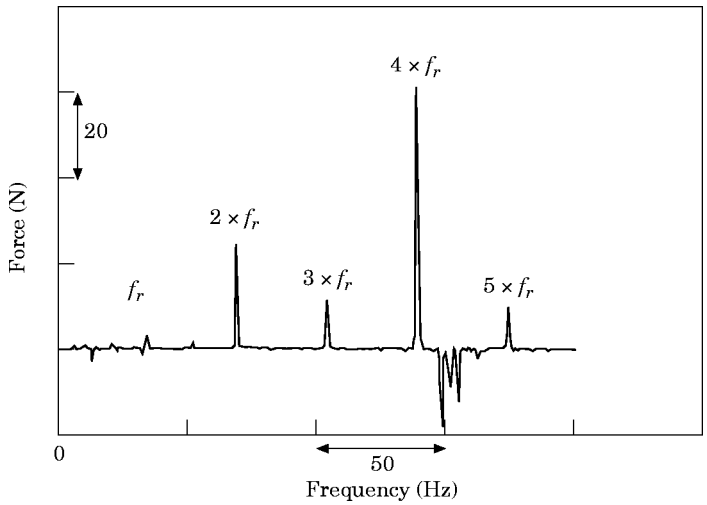

Figure 10. Measurement of the force generated by a parallel misalignment Δy at the journal on the "Motor" side.

4.1. VIBRATION COMPARISON

The vibration model developed in reference [1] leads to the evolution of natural frequencies as a function of the rotor running speed. Vibration responses to excitation forces characteristic of the defects are also obtained.

The main results from the comparison between the calculations and the experiments are the following.

1. The calculation of natural frequencies, and of the first two critical speeds from the values of the journal stiffnesses is adequate.

2. The present approach describes with accuracy the defect due to imbalance.

3. As far as misalignment is concerned, the comparison between acceleration and inertia measurements at the journals with respect to the displacement Δy of journal 1 (see Figure 5) and the accelerations calculated by the model (see Figure 8 of reference [1]) presented in the Appendix of the theoretical part ([1]) gave the following results (see Figures 11 and 12).

The magnitude variation of the component $2 \times f_r$ increases with the misalignment in both experimental and theoretical cases.

The variation of the fifth component $5 \times f_r$ seems to follow a parabolic increase in both cases.

Theory and experimental results are in contradiction for the fourth component $4 \times f_r$ on journal 2. This may be due to the simplifying hypotheses made in the theoretical model [3].

4.2. ACOUSTIC COMPARISON

One recalls that the structure consists of part II ("journals") which are acoustically isolated from the other two parts. The support, rotor and journals are the vibrating elements. Their geometry is so complex that it is difficult to apply

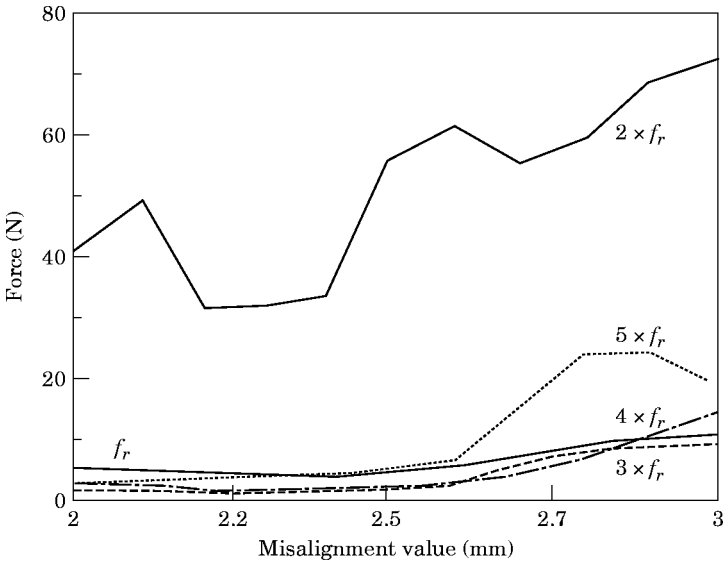

Figure 11. Measurement of the force at the journal on the "receptor" side for frequencies corresponding to harmonics of the rotation frequency as a function of Δy.

the model developed in the theoretical part [1]. To calculate the acoustic pressure, one uses (expression (23) of reference [1])

$$\tilde{P}(M) = \mathrm{j}\rho_0\omega \sum_{i=1}^{N_e} |V_i|\, \mathrm{e}^{j(\varphi_{ref} - \varphi_i)} G(M, M_i)\, \Delta S_i, \tag{1}$$

where $|V_i|\, \mathrm{e}^{j(\varphi_{ref} - \varphi_i)}$ is the vibrating speed expressed by its magnitude and phase at point i of the vibrating surface $S = \Sigma\, \Delta si$.

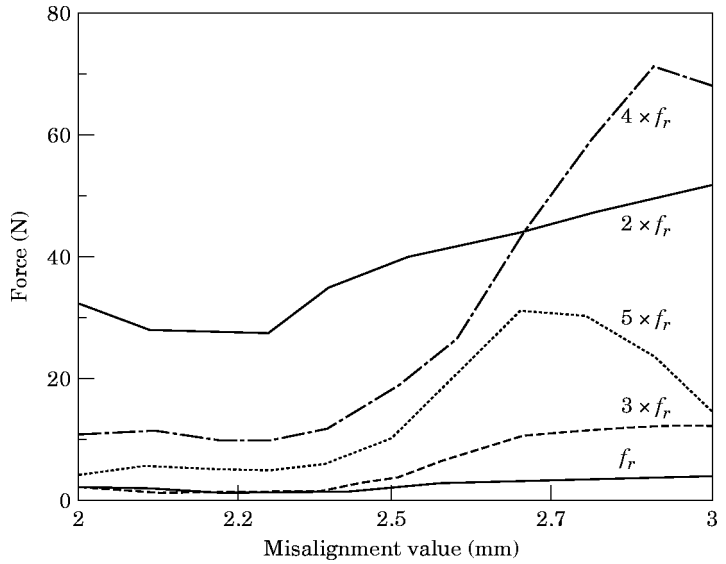

Figure 12. Measurement of the force at the journal on the "Motor" side for frequencies corresponding to harmonics of the rotation frequency as a function of Δy.

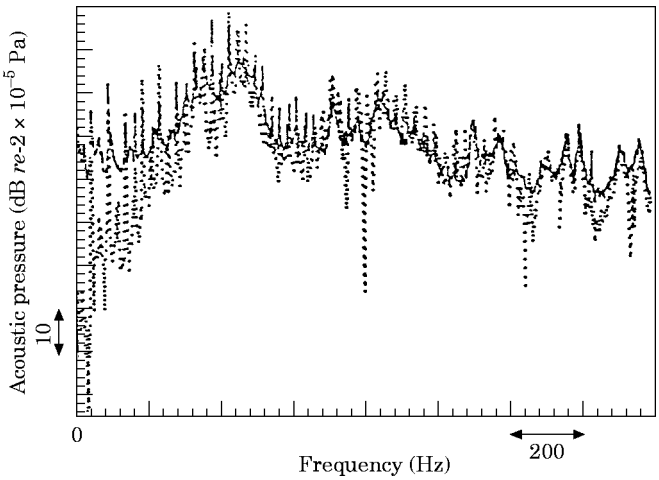

Figure 13. Acoustic pressure level radiated by part II. ——, Experiment; · · · · , theory (expression (1)).

$G(M, M_i) = (e^{-jkr_1}/4\pi r_1) + (e^{-jkr_2}/4\pi r_2)$ is the Green function describing the radiation of a structure placed in a semi-anechoic field [1]. The acoustic pressure calculated by expression (1) is not very accurate [4]. The error is due to theoretical simplifications (the dipolar effect was neglected, discretized integrals . . .) and to the quality of the measurements (mesh, consistency of measures . . .). One recalls that the first goal is to test the reliability of the present acoustic predictions from

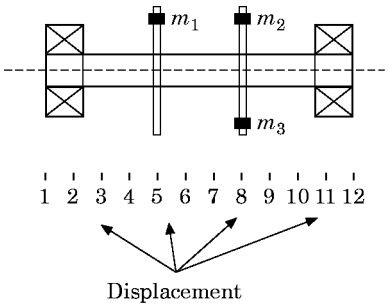

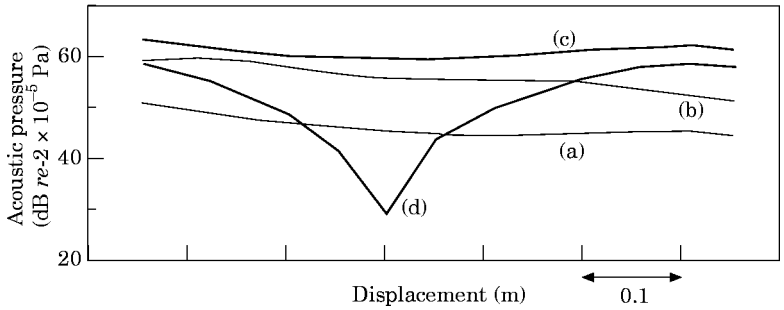

Figure 14. Acoustic pressure level spacial variations calculated for different kinds of imbalance at f_r. (a) Without defects; (b) imbalance (m_1); (c) imbalance ($m_1 + m_2$); (d) imbalance ($m_1 + m_3$).

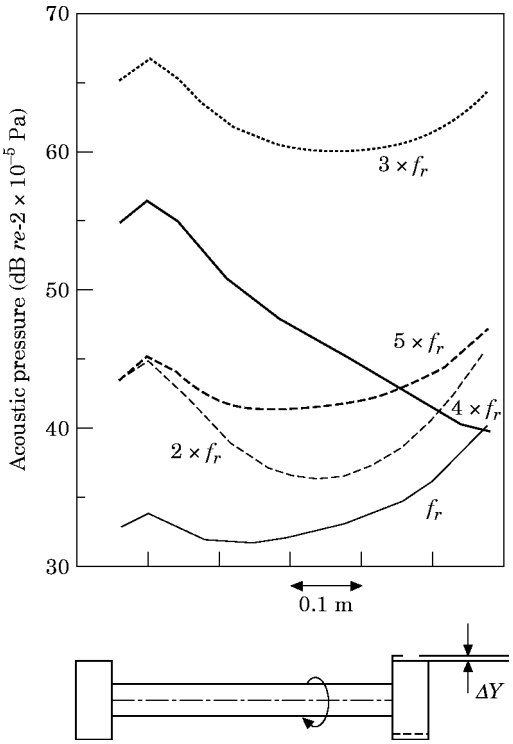

Figure 15. Acoustic pressure level spatial variations calculated at some harmonics of f_r, for a misalignment Δy.

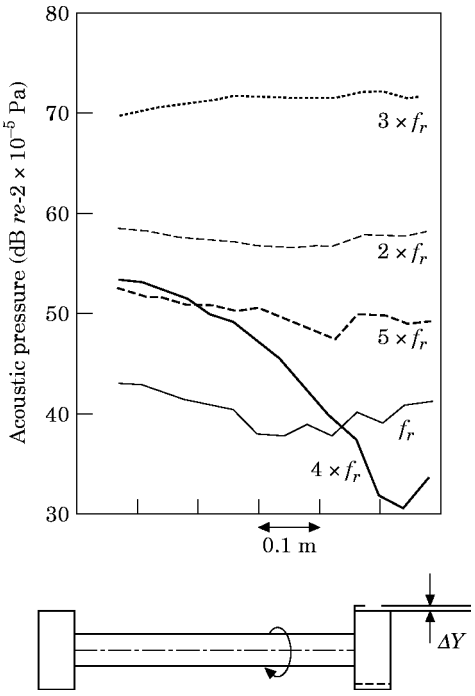

Figure 16. Acoustic pressure level spatial variations measured at some harmonics of f_r, for a misalignment Δy.

vibration measurements in order to characterise mechanical defects such as imbalance or misalignment through noise level analysis.

The main results relative to this part are the following.

From a 26 node mesh, the nodes being distributed on the support and the journals of part II, one compares the measured and calculated pressure. This comparison is satisfactory at the running frequency and its harmonics, and at the system natural frequencies in spite of the errors presented above (see Figure 13).

With two points on the two journals when vibration speeds (magnitude and phase) were measured, acoustic pressure variations calculated at the running frequency f_r for three types of imbalance (see Figure 14) were simulated. The results from the experiments are presented in Figure 7 and are similar to the ones obtained from the theoretical model. The same approach using measurements of vibration speeds calculated on the rotating axis and the two journals leads to the same results (see Figure 14 of reference [1]).

The same procedure was carried out with a misalignment defect instead of inbalance. It consists of expressing the variation of the acoustic pressure level harmonics as a function of the spacial position variable from one journal to another. The spacial variations obtained from the theoretical model and the experimental results were found to be approximately equal (see Figures 15 and 16). In the case of parallel misalignment of the journal, only the component $4 \times f_r$ seems to have a spacial variation of acoustic pressure, its level regularly decreases as the microphone moves from one journal to another.

5. CONCLUSIONS

A vibro–acoustic characterisation of imbalance and misalignment defects encountered in rotating machinery has been presented. A straightforward approach based on a linear model was used that was compared with experimental results. The results of this study suggest that a reverse approach should be taken in order to identify these defects by the means of a vibro–acoustic analysis.

The main points of the conclusion can be summarized as follows.

1. The prototype of the experimental installation shows that vibration and acoustic levels are low when the system is defect free; the relationship between the defects and noise generation is confirmed and should yield a definition of criteria for the acoustic quality of a machine.

2. Theoretical or experimental simulation of defects (imbalance or misalignment) can be acoustically characterised by the acoustic power or spacial variations of the pressure.

3. The application of theoretical simplified approaches in rotating machinery qualitatively describes the acoustic response of a machine but quantitative prediction of noise calculated from vibration measurements is inadequate. The accuracy is mainly due to phase variations between vibrating speeds and the type of acoustic field around the machine.

4. A perfect knowledge of the journals, their stiffness and clearance, is necessary to assess internal forces. A dynamic linear model can lead to the development of experimental procedures for detecting defects.

ACKNOWLEDGMENTS

This work is part of a project with the INRS Nancy and the Campagna & Varenne company. We also acknowledge the support of the Research and Technology Ministry and Work Ministry.

REFERENCES

1. N. Hamzaoui, C. Boisson and C. Lesueur 1998 *Journal of Sound and Vibration* **216**, 553–570. Vibro-acoustic analysis and identification of defects in rotating machinery, Part I: theoretical model.
2. N. Hamzaoui, C. Boisson, J. P. Thome and C. Millard 1992 *Progrès récents des méthodes de surveillance acoustiques et vibrations*, *conférence Internationale Senlis* 27–29 *octobre*. Apport et limitation de l'analyse acoustique pour l'identification des défauts de machines tourantes.
3. C. Fischer and V. Terrail 1993 *Rapport projet de fin d'etudes GMC INSA Lyon juin*. Etude vibroacoustique du mésalignement entre deux paliers.
4. N. Hamzaoui, C. Boisson and C. Lesueur 1992 *Journal de Physique* IV, *Colloque C*1, *Supplément au Journal de Physique* III **2**, 467–470. Prévision du bruit et diagnostic vibroacoustique d'un système composé d'un rotor sur deux paliers à roulements.